Shape-preserving interpolation of spatial data by Pythagorean-hodograph quintic spline curves

Shape-preserving interpolation of spatial data by Pythagorean-hodograph quintic spline curves

Rida T. Farouki*
Department of Mechanical and Aerospace Engineering,
University of California, Davis CA 95616, USA.

Carla Manni†
Dipartimento di Matematica, Università di Roma "Tor Vergata,"
Via della Ricerca Scientifica, 00133 Roma, Italy.

Maria Lucia Sampoli‡
Dipartimento di Ingegneria dell'Informazione e Scienze Matematiche,
Università di Siena, Pian dei Mantellini 44, 53100 Siena, Italy.

Alessandra Sestini§
Dipartimento di Matematica e Informatica, Università di Firenze,
Viale Morgagni 67/A, 50134 Firenze, Italy.

Abstract

The interpolation of discrete spatial data — a sequence of points and unit tangents — by G^1 Pythagorean–hodograph (PH) quintic spline curves, under shape constraints, is addressed. To achieve this, a local Hermite scheme incorporating a tension parameter for each spline segment is employed, the imposed shape constraints being concerned with preservation of convexity at the knots and the sign of the discrete torsion over each spline segment. An asymptotic analysis in terms of the tension parameters is developed, and it is shown that satisfaction of the prescribed shape constraints can always be achieved for each spline segment by a suitable choice of the free angular parameters that characterize each PH quintic Hermite segment. In particular, it is proved that the CC criterion ([12, 27]) for specifying these free parameters ensures satisfaction of the desired shape–preserving properties, requiring only mild application of the tension parameters that does not compromise the overall fairness of the interpolant. The performance of the method is illustrated through some computed examples.

*Email: farouki@ucdavis.edu
†Email: manni@mat.uniroma2.it
‡Email: marialucia.sampoli@unisi.it
§Email: alessandra.sestini@unifi.it

spatial Pythagorean–hodograph curves; shape–preserving interpolation; tension parameters; G^1 spline curves; Hermite interpolation; quaternions.

1 Introduction

The ability to preserve the shape suggested by discrete data is an important feature of planar and spatial spline interpolation schemes, in both the functional and parametric case. To address this requirement, several *shape–preserving interpolation schemes* (see the survey [18] and references therein) have been developed in recent decades, within the more general context of constrained interpolation — see, for example, [5, 22, 6].

Since classical polynomial or polynomial spline interpolants do not, in general, guarantee shape–preserving properties, new representations have been introduced, endowed with free parameters that can be adjusted to ensure satisfaction of the shape–preservation constraints. Among such methods, the well-known *tension schemes*, originally introduced for univariate functional interpolation, employ free parameters that can be used to make a smooth interpolant converge toward the piecewise–linear curve connecting the data points (which is inherently shape–preserving). While shape–preserving planar interpolation can be traced to the introduction of the exponential tension spline in [26], the development of shape–preserving interpolation algorithms for spatial data is more recent — see, for example, [20, 19, 21, 1, 3, 4, 25].

Polynomial *Pythagorean–hodograph* (PH) *curves* have the distinctive property that the parametric speed — i.e., the derivative of arc length with respect to the curve parameter — is simply a polynomial (rather than the square–root of a polynomial). This key property confers several important computational advantages on PH curves, in terms of arc length measurement, rational offset curves, real–time motion control, spatial path planning, etc. — see [8] for a short introduction, and [9] for a comprehensive treatment. The construction of planar PH curves is facilitated by a complex–number model ([7]), while models based on the quaternions or the Hopf map from $\mathbb{R}^4$ to $\mathbb{R}^3$ are used for spatial PH curves ([2, 11]). Efficient algorithms to compute planar C^2 PH quintic splines interpolating given points were developed in [13, 24], and shape–preserving G^1 and G^2 extensions of them were proposed in [15] based on a local and a global approach, respectively.

In the case of spatial curves, a scheme for local G^1 interpolation of "reasonable" Hermite data by PH cubics was described in [23]. Methods for interpolation of C^1 Hermite data by spatial PH quintics are also available ([10, 12, 28]) and have been generalized in [16, 14] to the case of C^2 splines interpolating a sequence of point data. In the case of interpolation by spatial PH quintics, two free angular parameters are associated with each spline segment, incurring underdetermined systems of equations. Since the values of these free parameters can strongly influence the shape of the interpolant, optimization strategies must be developed to ensure that they yield interpolants with desirable shape

properties. The treatment of these free parameters makes the development of shape–preserving spatial PH spline interpolation schemes, addressed herein for the first time, a much more challenging task than for the planar case treated in [15].

The focus of this study is on the development of a local method to construct a G^1 Hermite spatial PH quintic spline that interpolates at its knots an ordered sequence of points $\mathbf{p}_0, \ldots, \mathbf{p}_N$ and associated unit tangents $\mathbf{t}_0 \ldots, \mathbf{t}_N$ under shape constraints. Specifically, these constraints are imposed by defining discrete quantities in terms of the Hermite data — a left and right discrete binormal at each data point, and a discrete torsion for each segment — and then by requiring that at each knot the left and right spline binormals have a positive projection on the corresponding left and right discrete binormals, and that the sign of the torsion over each spline segment conforms to that of the related discrete torsion. The scheme is local in nature, based on local PH quintic Hermite interpolants. In cases where they do not hold initially, satisfaction of the shape constraints is achieved by adjustment of the tension parameters (one for each spline segment). In this local scheme, each spline segment incorporates two free angular parameters (besides the tension parameter), that can strongly influence the shape of the interpolant. An asymptotic analysis in terms of the tension parameter associated with each spline segment shows that the admissibility region for the free angular parameters (that ensures satisfaction of the prescribed shape constraints) is non–empty. In practice, the data–dependent CC criterion for assigning the free parameters — introduced in [12], and subsequently analyzed in terms of approximation order in [27] — is used, and it is proved that for reasonable data it ensures asymptotic satisfaction of the shape constraints. Furthermore, the numerical experiments show that this criterion is also advantageous in terms of shape quality, since it often requires only mild application of the tension parameters, that does not significantly alter the overall fairness of the resulting interpolant.

This paper is organized as follows. The spatial PH quintic spline Hermite interpolation problem under shape constraints is introduced in Section 2, and the construction and basic properties of spatial PH quintics are briefly reviewed in Section 3. Section 4 then discusses the local G^1 construction, and summarizes the CC criterion for selecting the free parameters. The asymptotic analysis with respect to the tension parameter is presented in Section 5, with special attention to the behavior of the interpolant defined by invoking the CC criterion. Several computed examples are reported in Section 6, which serve to illustrate the shape–preservation properties of the scheme. Finally, Section 7 summarizes the main results obtained herein, and identifies issues that deserve further investigation.

2 Spatial PH quintic spline interpolation with shape constraints

Let $\mathbf{p}_0, \ldots, \mathbf{p}_N$ be given points in $\mathbb{R}^3$ with $\mathbf{p}_j \neq \mathbf{p}_{j+1}$ and let $\mathbf{t}_0, \ldots, \mathbf{t}_N$ be given unit tangent vectors associated with those points. The goal is to construct a PH spline curve $\mathbf{S}(u)$ for $u \in [\, a, b\,]$ with assigned knots $a = u_0 < \cdots < u_N = b$ that interpolates the given data, i.e.,

$$\mathbf{S}(u_j) \;=\; \mathbf{p}_j \quad \text{and} \quad \frac{\mathbf{S}'(u_j)}{|\mathbf{S}'(u_j)|} \;=\; \mathbf{t}_j \qquad \text{for } \; j = 0, \ldots, N\,,$$

and also satisfies certain *shape constraints*. Let $[\, \mathbf{a}, \mathbf{b}, \mathbf{c}\,]$ denote the scalar triple product $(\mathbf{a} \times \mathbf{b}) \cdot \mathbf{c}$ of given vectors $\mathbf{a}, \mathbf{b}, \mathbf{c} \in \mathbb{R}^3$. In order to define the shape constraints, the following notations are introduced

$$\begin{aligned} \Delta\mathbf{p}_j \;&:=\; \mathbf{p}_{j+1} - \mathbf{p}_j\,, & \mathbf{N}_{j,i} \;&:=\; \tfrac{\mathbf{t}_j \times \Delta\mathbf{p}_j}{|\mathbf{t}_j \times \Delta\mathbf{p}_j|}\,, \\ \tau_j \;&:=\; \left[\, \mathbf{t}_j, \frac{\Delta\mathbf{p}_j}{|\Delta\mathbf{p}_j|}, \mathbf{t}_{j+1} \,\right] & \mathbf{N}_{j,f} \;&:=\; \tfrac{\Delta\mathbf{p}_j \times \mathbf{t}_{j+1}}{|\Delta\mathbf{p}_j \times \mathbf{t}_{j+1}|} \end{aligned} \tag{1}$$

for $j = 0, \ldots, N-1$. $\Delta\mathbf{p}_j$ is the displacement vector for the spline segment $u \in [\, u_j, u_{j+1}\,]$; $\mathbf{N}_{j,i}$ and $\mathbf{N}_{j,f}$ are the discrete binormals[1] at its end–points; and τ_j has the same sign as the discrete torsion for that segment ([20]). Now if $|\mathbf{S}'(u)| \neq 0$ and $|\mathbf{S}'(u) \times \mathbf{S}''(u)| \neq 0$, the *curvature vector* and *torsion* are defined by

$$\mathbf{k}_S(u) \;:=\; \frac{\mathbf{S}'(u) \times \mathbf{S}''(u)}{|\mathbf{S}'(u)|^3} \qquad \text{and} \qquad \tau_S(u) \;:=\; \frac{[\, \mathbf{S}'(u), \mathbf{S}''(u), \mathbf{S}'''(u)\,]}{|\mathbf{S}'(u) \times \mathbf{S}''(u)|^2}$$

for each segment $u \in (u_j, u_{j+1})$ of $\mathbf{S}(u)$, $j = 0, \ldots, N-1$. Note that $\mathbf{k}_S(u)$ is aligned with the binormal vector of $\mathbf{S}(u)$, and $|\mathbf{k}_S(u)|$ is the scalar curvature. In terms of these quantities, the shape constraints are defined as follows

- *convexity constraint* — if $\mathbf{N}_{j,i} \neq \mathbf{0}$, then $\lim_{u \to u_j^+} \mathbf{k}_S(u) \cdot \mathbf{N}_{j,i} > 0$, if $\mathbf{N}_{j,f} \neq \mathbf{0}$, then $\lim_{u \to u_{j+1}^-} \mathbf{k}_S(u) \cdot \mathbf{N}_{j,f} > 0$,
- *torsion constraint* — if $\tau_j \neq 0$, then $\tau_S(u)\, \tau_j > 0$ for $u \in [\, u_j^+, u_{j+1}^-\,]$.

The requirement that a property should hold for $u \in [\, u_j^+, u_{j+1}^-\,]$ means that it holds on the open interval (u_j, u_{j+1}) and as a left and right limit at the end–points of the interval. Note that, since unit tangents are asssumed as input data, these shape–preserving criteria are actually a subset of those usually considered in the literature (e.g., [21, 1]), as the convexity constraints are relaxed herein.

[1] It is assumed that $\mathbf{N}_{j,i} := \mathbf{0}$ if $|\mathbf{t}_j \times \Delta\mathbf{p}_j| = 0$, and $\mathbf{N}_{j,f} := \mathbf{0}$ if $|\Delta\mathbf{p}_j \times \mathbf{t}_{j+1}| = 0$.

3 Properties of spatial PH quintics

A spatial Pythagorean–hodograph (PH) curve $\mathbf{r}(t)$, $t \in [\,0,1\,]$ can be constructed from a quaternion[2] polynomial $\mathcal{A}(t) = u(t) + v(t)\,\mathbf{i} + p(t)\,\mathbf{j} + q(t)\,\mathbf{k}$ and its conjugate $\mathcal{A}^*(t) = u(t) - v(t)\,\mathbf{i} - p(t)\,\mathbf{j} - q(t)\,\mathbf{k}$ by integrating the derivative or *hodograph* $\dot{\mathbf{r}}(t) = (\dot{x}(t), \dot{y}(t), \dot{z}(t))$ specified by the product

$$\dot{\mathbf{r}}(t) \;:=\; \mathcal{A}(t)\,\mathbf{u}\,\mathcal{A}^*(t)\,, \tag{2}$$

where $\mathbf{u}$ is a unit vector and dots denote derivatives with respect to the local parameter t. The components of $\dot{\mathbf{r}}(t)$ satisfy the Pythagorean condition

$$\dot{x}^2(t) + \dot{y}^2(t) + \dot{z}^2(t) \;=\; \sigma(t)\,,$$

where the polynomial

$$\sigma(t) \;=\; |\dot{\mathbf{r}}(t)| \;=\; |\mathcal{A}(t)|^2 \;=\; u^2(t) + v^2(t) + p^2(t) + q^2(t) \tag{3}$$

is the *parametric speed* of $\mathbf{r}(t)$, i.e., the derivative of its arc length with respect to the parameter t. Integration of (2) yields a spatial PH curve $\mathbf{r}(t)$ of degree $n = 2m+1$, if $\mathcal{A}(t)$ is of degree m.

The lowest–order spatial PH curves capable of first–order Hermite interpolation are the quintics, generated by quadratic quaternion polynomials specified in Bernstein form as

$$\mathcal{A}(t) \;:=\; \mathcal{A}_0(1-t)^2 \;+\; \mathcal{A}_1 2(1-t)t \;+\; \mathcal{A}_2 t^2\,. \tag{4}$$

Integrating the hodograph defined by substituting (4) into (2) yields the Bézier form

$$\mathbf{r}(t) \;:=\; \sum_{k=0}^{5} \mathbf{q}_k\, b_k^5(t)\,, \quad t \in [\,0,1\,] \tag{5}$$

of the PH quintic, where the degree–n Bernstein basis functions are defined by

$$b_k^n(t) \;:=\; \binom{n}{k}(1-t)^{n-k}t^k\,, \quad k = 0,\ldots,n\,,$$

and the control points $\mathbf{q}_0,\ldots,\mathbf{q}_5$ of (5) are given in terms of the coefficients of (4) by

$$\begin{aligned}
\mathbf{q}_1 \;&:=\; \mathbf{q}_0 \;+\; \tfrac{1}{5}\,\mathcal{A}_0\,\mathbf{u}\,\mathcal{A}_0^*\,,\\
\mathbf{q}_2 \;&:=\; \mathbf{q}_1 \;+\; \tfrac{1}{10}(\mathcal{A}_0\,\mathbf{u}\,\mathcal{A}_1^* + \mathcal{A}_1\,\mathbf{u}\,\mathcal{A}_0^*)\,,\\
\mathbf{q}_3 \;&:=\; \mathbf{q}_2 \;+\; \tfrac{1}{30}(\mathcal{A}_0\,\mathbf{u}\,\mathcal{A}_2^* + 4\,\mathcal{A}_1\,\mathbf{u}\,\mathcal{A}_1^* + \mathcal{A}_2\,\mathbf{u}\,\mathcal{A}_0^*)\,,\\
\mathbf{q}_4 \;&:=\; \mathbf{q}_3 \;+\; \tfrac{1}{10}(\mathcal{A}_1\,\mathbf{u}\,\mathcal{A}_2^* + \mathcal{A}_2\,\mathbf{u}\,\mathcal{A}_1^*)\,,\\
\mathbf{q}_5 \;&:=\; \mathbf{q}_4 \;+\; \tfrac{1}{5}\,\mathcal{A}_2\,\mathbf{u}\,\mathcal{A}_2^*\,.
\end{aligned} \tag{6}$$

[2] Calligraphic characters such as $\mathcal{A}$ denote quaternions, the scalar and vector parts being indicated by scal($\mathcal{A}$) and vect($\mathcal{A}$). A synopsis of the quaternion algebra may be found in Section 2 of [12]. Bold characters denote vectors in $\mathbb{R}^3$.

A PH quintic is thus completely specified by the three quaternion coefficients $\mathcal{A}_0$, $\mathcal{A}_1$, $\mathcal{A}_2$ and the initial control point $\mathbf{q}_0$. However, for any quaternion $\mathcal{U} = \exp(\theta\,\mathbf{u}) := \cos\theta + \sin\theta\,\mathbf{u}$ satisfying $\mathcal{U}\,\mathbf{u}\,\mathcal{U}^* = \mathbf{u}$, the quaternion polynomial $\mathcal{B}(t) = \mathcal{A}(t)\mathcal{U}$ also generates the hodograph (2) — see [11]. Hence, one of the 12 degrees of freedom embodied in $\mathcal{A}_0$, $\mathcal{A}_1$, $\mathcal{A}_2$ is redundant.

The parametric speed (3) of the PH quintic defined by (2) and (4) can be expressed as

$$\sigma(t) \;=\; |\mathcal{A}(t)|^2 \;=\; \sum_{k=0}^{4} \sigma_k\, b_k^4(t)\,, \tag{7}$$

with the quartic Bernstein coefficients

$$\begin{aligned} \sigma_0 \;&:=\; |\mathcal{A}_0|^2\,, \quad \sigma_1 \;=\; \tfrac{1}{2}(\mathcal{A}_0\,\mathcal{A}_1^* + \mathcal{A}_1\,\mathcal{A}_0^*)\,, \\ \sigma_2 \;&:=\; \tfrac{1}{6}(\mathcal{A}_0\,\mathcal{A}_2^* + 4\,|\mathcal{A}_1|^2 + \mathcal{A}_2\,\mathcal{A}_0^*)\,, \\ \sigma_3 \;&:=\; \tfrac{1}{2}(\mathcal{A}_1\,\mathcal{A}_2^* + \mathcal{A}_2\,\mathcal{A}_1^*)\,, \quad \sigma_4 \;=\; |\mathcal{A}_2|^2\,. \end{aligned} \tag{8}$$

Consequently, the total arc length of this PH quintic is given by

$$L \;:=\; \int_0^1 \sigma(t)\;\mathrm{d}t \;=\; \frac{\sigma_0 + \sigma_1 + \sigma_2 + \sigma_3 + \sigma_4}{5}\,. \tag{9}$$

4 Local G^1 scheme based on PH quintics with tension

The approach considered here is a local G^1 scheme, based on spatial PH quintics. Each segment $u \in [\,u_j,\,u_{j+1}\,]$ of $\mathbf{S}(u)$ is independently defined, and parameterized in terms of the local variable

$$t \;:=\; \frac{u - u_j}{u_{j+1} - u_j} \;\in\; [\,0,1\,]\,.$$

Since the method is local in nature, it suffices to focus henceforth on the j–th spline segment. Denoting this segment by $\mathbf{r}(t)$, and its end points and tangents $\mathbf{p}_j$, $\mathbf{p}_{j+1}$ and $\mathbf{t}_j$, $\mathbf{t}_{j+1}$ by $\mathbf{p}_i$, $\mathbf{p}_f$ and $\mathbf{t}_i$, $\mathbf{t}_f$ it must satisfy the local Hermite interpolation conditions

$$\mathbf{r}(0) \;=\; \mathbf{p}_i\,, \quad \dot{\mathbf{r}}(0) \;=\; s^2\lambda_i\,\mathbf{t}_i\,, \qquad \text{and} \qquad \mathbf{r}(1) \;=\; \mathbf{p}_f\,, \quad \dot{\mathbf{r}}(1) \;=\; s^2\lambda_f\,\mathbf{t}_f\,, \tag{10}$$

where λ_i, λ_f and s are positive free parameters, and dots denote derivatives with respect to the local parameter t. Note that, without loss of generality, one can assume $\lambda_i^2 + \lambda_f^2 = c$ for any positive constant c, so there are only two independent parameters in (10) that influence the shape of the local interpolant: the ratio λ_f/λ_i and the value s — the former determines the ratio of the initial and final parametric speeds of the PH quintic segment, while the latter controls their magnitudes. To make the scheme more automatic, a strategy is proposed in Section 6 below to fix a reasonable value for the ratio λ_f/λ_i, while s is used

as a free parameter that causes the interpolant to converge on the line segment joining $\mathbf{p}_i$ and $\mathbf{p}_f$ as $s \to 0$. In practice, an initial reasonable s value is selected, and it is reduced only when necessary to guarantee satisfaction of the prescribed shape–preserving criteria (see Section 6). For brevity, the quantities (1) for the generic j–th segment will henceforth be denoted by $\Delta\mathbf{p}$, $\mathbf{N}_i$, $\mathbf{N}_f$, and τ.

4.1 PH quintic Hermite interpolation

The interpolation conditions (10) are satisfied ([10, 12]) by choosing $\mathbf{q}_0 = \mathbf{p}_i$ and specifying $\mathcal{A}_0$, $\mathcal{A}_1$, $\mathcal{A}_2$ in the form

$$\mathcal{A}_0 := s\sqrt{\lambda_i}\,\mathcal{U}_0\,, \quad \mathcal{A}_1 := \tfrac{1}{4}\,\mathcal{D} - \tfrac{3}{4}\,s\left[\sqrt{\lambda_i}\,\mathcal{U}_0 + \sqrt{\lambda_f}\,\mathcal{U}_2\right], \quad \mathcal{A}_2 := s\sqrt{\lambda_f}\,\mathcal{U}_2\,, \tag{11}$$

where the unit quaternions $\mathcal{U}_0, \mathcal{U}_2$ and non–unit quaternion $\mathcal{D}$ satisfy the three (vector) equations

$$\mathcal{U}_0\,\mathbf{u}\,\mathcal{U}_0^* = \mathbf{t}_i\,, \qquad \mathcal{U}_2\,\mathbf{u}\,\mathcal{U}_2^* = \mathbf{t}_f\,, \qquad \mathcal{D}\,\mathbf{u}\,\mathcal{D}^* = \mathbf{d}\,, \tag{12}$$

with the vector $\mathbf{d}$ being defined by

$$\mathbf{d} := 120\,\Delta\mathbf{p} + s^2\left[5\sqrt{\lambda_i\,\lambda_f}\,(\mathcal{U}_0\,\mathbf{u}\,\mathcal{U}_2^* + \mathcal{U}_2\,\mathbf{u}\,\mathcal{U}_0^*) - 15\,(\lambda_i\,\mathbf{t}_i + \lambda_f\,\mathbf{t}_f)\right]. \tag{13}$$

The first two equations in (12) have solutions of the form

$$\mathcal{U}_0 := \mathbf{n}_i\,\exp((\alpha - \tfrac{1}{2}\beta)\,\mathbf{u})\,, \qquad \mathcal{U}_2 := \mathbf{n}_f\,\exp((\alpha + \tfrac{1}{2}\beta)\,\mathbf{u})\,, \tag{14}$$

where α, β are free angular parameters, and

$$\mathbf{n}_i := \frac{\mathbf{u} + \mathbf{t}_i}{|\,\mathbf{u} + \mathbf{t}_i\,|}\,, \qquad \mathbf{n}_f := \frac{\mathbf{u} + \mathbf{t}_f}{|\,\mathbf{u} + \mathbf{t}_f\,|} \tag{15}$$

are the unit bisectors of $\mathbf{u}$, $\mathbf{t}_i$ and $\mathbf{u}$, $\mathbf{t}_f$. As observed in [12], the free parameters α and β can strongly influence the shape of the PH quintic Hermite interpolant. In this regard, it is interesting to note ([12]) that the arc length of the PH quintic Hermite interpolant depends only on β. Moreover, if β is fixed and an admissible arc length is thus determined, the appropriate selection of α is often crucial to ensure a reasonable control polygon through equations (6) and (11)–(17).

Since (as noted above), the coefficients $\mathcal{A}_0$, $\mathcal{A}_1$, $\mathcal{A}_2$ incorporate one redundant degree of freedom, one may assume without loss of generality that $\mathrm{scal}(\mathcal{D}) = 0$, and the third equation in (12) then has the solution

$$\mathcal{D} := \sqrt{|\mathbf{d}|}\,\mathbf{n}\,, \tag{16}$$

with $\mathbf{n}$ being the unit bisector of $\mathbf{u}$ and a unit vector in the direction of $\mathbf{d}$, namely

$$\mathbf{n} := \frac{\mathbf{u} + \mathbf{t}}{|\,\mathbf{u} + \mathbf{t}\,|}\,, \quad \text{where } \mathbf{t} := \frac{\mathbf{d}}{|\,\mathbf{d}\,|}\,. \tag{17}$$

For the asymptotic analysis developed in the following section, it will be convenient (see [12]) to re–write the vector (13) as

$$\mathbf{d} \;=\; \mathbf{d}^{(0)} \;+\; s^2\,\mathbf{d}^{(2)}\,, \tag{18}$$

where

$$\mathbf{d}^{(0)} \;=\; 120\,\Delta\mathbf{p}\,, \qquad \mathbf{d}^{(2)} \;=\; 10\,\sqrt{\lambda_i\lambda_f}(\mathbf{e}\,\cos\beta + \mathbf{f}\,\sin\beta) \;-\; 15\,(\lambda_i\,\mathbf{t}_i + \lambda_f\,\mathbf{t}_f)\,, \tag{19}$$

with the vectors $\mathbf{e}$ and $\mathbf{f}$ being defined as

$$\mathbf{e} \;:=\; \frac{(1+\mathbf{u}\cdot\mathbf{t}_f)\,\mathbf{t}_i + (1+\mathbf{u}\cdot\mathbf{t}_i)\,\mathbf{t}_f + (1-\mathbf{t}_i\cdot\mathbf{t}_f)\,\mathbf{u}}{|\mathbf{u}+\mathbf{t}_i|\,|\mathbf{u}+\mathbf{t}_f|}\,,\; \mathbf{f} \;:=\; \frac{(\mathbf{t}_f-\mathbf{t}_i)\times\mathbf{u} - \mathbf{t}_i\times\mathbf{t}_f}{|\mathbf{u}+\mathbf{t}_i|\,|\mathbf{u}+\mathbf{t}_f|}\,. \tag{20}$$

4.2 Local shape control

From the properties of the Bernstein basis, one can verify that the convexity criterion of Section 2 is locally satisfied if and only if

$$[\,\mathbf{q}_1-\mathbf{q}_0\,,\,\mathbf{q}_2-\mathbf{q}_1\,,\,\mathbf{N}_i\,] \;>\; 0 \qquad \text{and} \qquad [\,\mathbf{q}_4-\mathbf{q}_3\,,\,\mathbf{q}_5-\mathbf{q}_4\,,\,\mathbf{N}_f\,] \;>\; 0\,. \tag{21}$$

For the torsion criterion, we require that

$$[\,\mathbf{q}_k-\mathbf{q}_{k-1}, \mathbf{q}_{k+1}-\mathbf{q}_k, \mathbf{q}_{k+2}-\mathbf{q}_{k+1}\,]\,\tau \;>\; 0 \quad k=1,2,3, \qquad \text{if } \tau \neq 0\,. \tag{22}$$

We recall (see, for example, [17, Example 7]) that the number of sign changes in the torsion of $\mathbf{r}(t)$ is bounded by the number of sign changes in the discrete torsion of its control polygon if there exists a (not necessarily orthogonal) strictly–convex projection of the control polygon onto some plane. However, this is not a problem for quintics. In fact, if the conditions (22) hold, it can be shown that a non–vanishing vector $\mathbf{v}$ exists, such that the control polygon has a strictly convex projection onto the plane orthogonal to $\mathbf{v}$. The following general result can be used to prove this fact.

Proposition 1. *Let* $\mathbf{g}_1,\ldots,\mathbf{g}_5$ *be vectors such that*

$$[\,\mathbf{g}_i\,,\,\mathbf{g}_{i+1}\,,\,\mathbf{g}_{i+2}\,] \;>\; 0 \quad \textit{for } i=1,2,3\,. \tag{23}$$

Then a vector $\mathbf{v}$ *exists, such that*

$$[\,\mathbf{g}_i\,,\,\mathbf{g}_{i+1}\,,\mathbf{v}\,] \;>\; 0 \quad \textit{for } i=1,2,3,4\,. \tag{24}$$

Proof : For suitable positive constants ϵ_1,ϵ_2 we define

$$\mathbf{v} \;:=\; \mathbf{g}_3 \;+\; \epsilon_1\,\mathbf{g}_2\times\mathbf{g}_3 \;+\; \epsilon_2\,\mathbf{g}_3\times\mathbf{g}_4\,.$$

Note that the second condition in (23) implies that $\mathbf{g}_2\times\mathbf{g}_3$ and $\mathbf{g}_3\times\mathbf{g}_4$ are linearly independent. Now by selecting ϵ_1,ϵ_2 suitably small, the first and third

conditions in (23) imply satisfaction of instances $i = 1$ and $i = 4$ of the inequalities (24). One can easily see that instances $i = 2$ and $i = 3$ are satisfied for any choice of the positive constants ϵ_1, ϵ_2 if $(\mathbf{g}_2 \times \mathbf{g}_3) \cdot (\mathbf{g}_3 \times \mathbf{g}_4) \geq 0$. If this is not the case, their satisfaction is ensured by requiring the ratio ϵ_1/ϵ_2 to satisfy the bounds

$$\frac{|(\mathbf{g}_2 \times \mathbf{g}_3) \cdot (\mathbf{g}_3 \times \mathbf{g}_4)|}{|(\mathbf{g}_2 \times \mathbf{g}_3)|^2} \;<\; \frac{\epsilon_1}{\epsilon_2} \;<\; \frac{|(\mathbf{g}_3 \times \mathbf{g}_4)|^2}{|(\mathbf{g}_2 \times \mathbf{g}_3) \cdot (\mathbf{g}_3 \times \mathbf{g}_4)|}\,,$$

which are admissible due to the Cauchy–Schwartz inequality and the linear independence of $\mathbf{g}_2 \times \mathbf{g}_3$ and $\mathbf{g}_3 \times \mathbf{g}_4$. Hence, $\mathbf{v}$ can always be chosen such that conditions (24) hold. ∎

4.3 The CC criterion

The CC (cubic–cubic) criterion was introduced in [12] as a simple means of choosing the free angles α, β using analytic data–dependent expressions that generally produce interpolants of good shape quality. The approximation order of this approach has recently been analyzed in greater detail in [27]. The method ensures that the PH quintic interpolant to given first–order Hermite data coincides with the "ordinary" cubic interpolant when it is a PH curve, and may be briefly summarized as follows (for complete details, see[3] [12]). First, the angle β is uniquely determined by solving the vector equation

$$\mathbf{e}\cos\beta \;+\; \mathbf{f}\sin\beta \;=\; \frac{1}{s^2\sqrt{\lambda_i\lambda_f}}\,\mathbf{w}_h\,, \tag{25}$$

where $\mathbf{e}$ and $\mathbf{f}$ are the vectors defined in (20), which belong to the plane Π orthogonal to $\mathbf{t}_f - \mathbf{t}_i$ (see [12]), and $\mathbf{w}_h$ is a suitable scaling[4] of the projection of the vector

$$\mathbf{w} \;:=\; 3\,\Delta\mathbf{p} \;-\; s^2(\lambda_i\,\mathbf{t}_i + \lambda_f\,\mathbf{t}_f) \tag{26}$$

onto the plane Π. To analyze the asymptotic behavior of the CC criterion, it is convenient to introduce the right–handed system of mutually orthogonal unit vectors

$$\mathbf{g}^- \;:=\; \frac{\mathbf{t}_f - \mathbf{t}_i}{|\mathbf{t}_f - \mathbf{t}_i|}\,, \quad \mathbf{g}^+ \;:=\; \frac{\mathbf{t}_i + \mathbf{t}_f}{|\mathbf{t}_i + \mathbf{t}_f|}\,, \quad \hat{\mathbf{g}} \;:=\; \frac{\mathbf{t}_i \times \mathbf{t}_f}{|\mathbf{t}_i \times \mathbf{t}_f|}\,, \tag{27}$$

which is well–defined for non–planar data. The vector on the right in (25) can then be written as

$$\frac{1}{s^2\sqrt{\lambda_i\lambda_f}}\,\mathbf{w}_h \;:=\; \frac{|\mathbf{t}_i \times \mathbf{t}_f|}{\sqrt{(\mathbf{w}_p \cdot \mathbf{g}^+)^2\,|\mathbf{t}_i \times \mathbf{t}_f|^2 + (\mathbf{w}_p \cdot \hat{\mathbf{g}})^2\,|\mathbf{t}_i + \mathbf{t}_f|^2}}\,\mathbf{w}_p\,, \tag{28}$$

where

$$\mathbf{w}_p \;:=\; \mathbf{w} \;-\; (\mathbf{w} \cdot \mathbf{g}^-)\,\mathbf{g}^-\,. \tag{29}$$

[3] Note however that the analysis in [12] is made under the assumption $\mathbf{u} = \mathbf{t}_i$.

[4] This scaling is necessary because, as β varies, the vector on the left in (25) describes an ellipse in the plane Π.

The CC criterion ([12]) proceeds by first determining a value for β, and then identifying a corresponding α value from the conditions

$$\tan\alpha \;=\; \frac{a\,\tan\frac{1}{2}\beta - b}{c + d\,\tan\frac{1}{2}\beta}\,, \qquad (c + d\,\tan\tfrac{1}{2}\beta)\,\cos\alpha + (a\,\tan\tfrac{1}{2}\beta - b)\,\sin\alpha \;>\; 0\,, \tag{30}$$

where

$$\begin{cases} a := (\sqrt{\lambda_i}\,\mathbf{n}_i - \sqrt{\lambda_f}\,\mathbf{n}_f)\cdot\mathbf{n}\,, & b := (\sqrt{\lambda_i}\,(\mathbf{u}\times\mathbf{n}_i) + \sqrt{\lambda_f}\,(\mathbf{u}\times\mathbf{n}_f))\cdot\mathbf{n}\,, \\ c := (\sqrt{\lambda_i}\,\mathbf{n}_i + \sqrt{\lambda_f}\,\mathbf{n}_f)\cdot\mathbf{n}\,, & d := (\sqrt{\lambda_i}\,(\mathbf{u}\times\mathbf{n}_i) - \sqrt{\lambda_f}\,(\mathbf{u}\times\mathbf{n}_f))\cdot\mathbf{n}\,. \end{cases} \tag{31}$$

Since the conditions (30) depend only on $\tan\frac{1}{2}\beta$ one may assume, without loss of generality, that

$$\cos\tfrac{1}{2}\beta \;>\; 0\,. \tag{32}$$

In the following section we first show that it is possible to select the free angles α, β so as to produce a shape–preserving interpolant when the tension parameter s is sufficiently small, and we then also prove that the CC criterion produces PH quintic spline interpolants which are asymptotically shape–preserving, in the sense specified in Section 2.

5 Asymptotic analysis

5.1 Asymptotic existence of shape–preserving interpolants

Based on the above results, the behavior of the local control polygon $\mathbf{q}_0, \ldots, \mathbf{q}_5$ is now studied as the tension parameter introduced in (10) satisfies $s \to 0$, beginning with the following preliminary result.

Proposition 2. *The total arc length (9) of the PH quintic segment* $\mathbf{r}(t)$*,* $t \in [\,0, 1\,]$ *satisfies* $L \to |\Delta\mathbf{p}|$ *as* $s \to 0$*, regardless of the values of the free parameters* α *and* β*.*

Proof. From (11), (14), and (16), the total arc length (9) can be expressed as

$$L \;=\; \frac{|\mathbf{d}| + 5\,s^2\,\big[\,6 - \sqrt{\lambda_i\,\lambda_f}\,(\mathcal{U}_0\,\mathcal{U}_2^* + \mathcal{U}_2\,\mathcal{U}_0^*)\,\big]}{120}\,, \tag{33}$$

where $|\mathbf{d}| \to 120\,|\Delta\mathbf{p}|$ as $s \to 0$ from (13). ∎

To obtain a more detailed analysis of the limit behavior of the curve as the tension parameter tends to zero, the directions of the control polygon legs $\mathbf{q}_k - \mathbf{q}_{k-1}$ for $k = 1, \ldots, 5$ must be investigated as $s \to 0$. For this purpose the analysis may be simplified, without loss of generality, by assuming that

$$\mathbf{u} \;=\; \frac{\Delta\mathbf{p}}{|\,\Delta\mathbf{p}\,|}\,. \tag{34}$$

For brevity, the angles $\phi_0, \phi_2 \in (-\pi, \pi\,]$ defined by

$$\phi_0 \,:=\, \alpha - \tfrac{1}{2}\beta\,, \qquad \phi_2 \,:=\, \alpha + \tfrac{1}{2}\beta\,, \tag{35}$$

are introduced. Writing

$$\mathcal{U}_0(\phi_0) \,=\, (u_i(\phi_0), \mathbf{u}_i(\phi_0)) \qquad \text{and} \qquad \mathcal{U}_2(\phi_2) \,=\, (u_f(\phi_2), \mathbf{u}_f(\phi_2))\,, \tag{36}$$

it follows from (1), (14), (15), and (34) that

$$\begin{array}{rcl} \mathbf{u}_i(\phi_0) & = & [(\mathbf{u}+\mathbf{t}_i)\,\cos\phi_0 + |\,\mathbf{u}\times\mathbf{t}_i\,|\,\mathbf{N}_i \sin\phi_0]/|\,\mathbf{u}+\mathbf{t}_i\,|\,, \\ \mathbf{u}_f(\phi_2) & = & [(\mathbf{u}+\mathbf{t}_f)\,\cos\phi_2 + |\,\mathbf{u}\times\mathbf{t}_f\,|\,\mathbf{N}_f \sin\phi_2]/|\,\mathbf{u}+\mathbf{t}_f\,|\,. \end{array} \tag{37}$$

Now the expression (18) for $\mathbf{d}$ implies that the quaternion (16) is of the form

$$\mathcal{D} \,=\, \sqrt{120\,|\Delta\mathbf{p}|}\;\mathbf{u} \,+\, O(s^2)\,. \tag{38}$$

Consequently, we have

$$\mathcal{A}_0 \,=\, s\,\sqrt{\lambda_i}\,\mathcal{U}_0\,, \quad \mathcal{A}_1 \,=\, \mathcal{A}_1^{(0)} + s\,\mathcal{A}_1^{(1)} + O(s^2)\,, \quad \mathcal{A}_2 \,=\, s\,\sqrt{\lambda_f}\,\mathcal{U}_2\,, \tag{39}$$

where

$$\mathcal{A}_1^{(0)} \,:=\, \tfrac{1}{2}\,\sqrt{30\,|\Delta\mathbf{p}|}\;\mathbf{u}\,, \quad \mathcal{A}_1^{(1)} \,:=\, -\tfrac{3}{4}\,(\sqrt{\lambda_i}\,\mathcal{U}_0 \,+\, \sqrt{\lambda_f}\,\mathcal{U}_2)\,, \tag{40}$$

and hence

$$\begin{array}{rcl} \mathcal{A}_0\,\mathbf{u}\,\mathcal{A}_1^* & = & \sqrt{\lambda_i}\,\Big[\,s\,\mathcal{U}_0\,\mathbf{u}\,\mathcal{A}_1^{(0)*} \,+\, s^2\,\mathcal{U}_0\,\mathbf{u}\,\mathcal{A}_1^{(1)*} \,+\, O(s^3)\Big]\,, \\ \mathcal{A}_1\,\mathbf{u}\,\mathcal{A}_1^* & = & \mathcal{A}_1^{(0)}\,\mathbf{u}\,\mathcal{A}_1^{(0)*} \,+\, s\,(\mathcal{A}_1^{(0)}\,\mathbf{u}\,\mathcal{A}_1^{(1)*} \,+\, \mathcal{A}_1^{(1)}\,\mathbf{u}\,\mathcal{A}_1^{(0)*}) \,+\, O(s^2)\,, \\ \mathcal{A}_1\,\mathbf{u}\,\mathcal{A}_2^* & = & \sqrt{\lambda_f}\,\Big[\,s\,\mathcal{A}_1^{(0)}\,\mathbf{u}\,\mathcal{U}_2^* \,+\, s^2\,\mathcal{A}_1^{(1)}\,\mathbf{u}\,\mathcal{U}_2^* \,+\, O(s^3)\Big]\,, \end{array} \tag{41}$$

where

$$\begin{array}{rcl} \mathcal{U}_0\,\mathbf{u}\,\mathcal{A}_1^{(0)*} & = & \tfrac{1}{2}\sqrt{30\,|\Delta\mathbf{p}|}\,(u_i(\phi_0), \mathbf{u}_i(\phi_0))\,, \\ \mathcal{A}_1^{(0)}\mathbf{u}\,\mathcal{A}_1^{(0)*} & = & \tfrac{15}{2}\,|\Delta\mathbf{p}|\;\mathbf{u}\,, \\ \mathcal{A}_1^{(0)}\mathbf{u}\,\mathcal{U}_2^* & = & \tfrac{1}{2}\sqrt{30\,|\Delta\mathbf{p}|}\,(u_f(\phi_2), \mathbf{u}_f(\phi_2))\,. \end{array}$$

The control points (6) can then be expressed as

$$\begin{array}{rcl} \mathbf{q}_1 - \mathbf{q}_0 & = & \tfrac{1}{5}\,s^2\,\lambda_i\,\mathbf{t}_i\,, \\ \mathbf{q}_2 - \mathbf{q}_1 & = & \tfrac{1}{10}\,\sqrt{\lambda_i}\,\Big[\,\sqrt{30\,|\Delta\mathbf{p}|}\;\mathbf{u}_i(\phi_0)\,s \,+\, 2\,\mathrm{vect}(\mathcal{U}_0\,\mathbf{u}\,\mathcal{A}_1^{(1)*})\,s^2 \,+\, O(s^3)\Big]\,, \\ \mathbf{q}_3 - \mathbf{q}_2 & = & \tfrac{1}{30}\,\Big[\,30\,|\Delta\mathbf{p}|\,\mathbf{u} \,+\, 8\,\mathrm{vect}(\mathcal{A}_1^{(0)}\,\mathbf{u}\,\mathcal{A}_1^{(1)*})\;s \,+\, O(s^2)\Big]\,, \\ \mathbf{q}_4 - \mathbf{q}_3 & = & \tfrac{1}{10}\,\sqrt{\lambda_f}\,\Big[\,\sqrt{30\,|\Delta\mathbf{p}|}\;\mathbf{u}_f(\phi_2)\,s \,+\, 2\,\mathrm{vect}(\mathcal{U}_2\,\mathbf{u}\,\mathcal{A}_1^{(1)*})\,s^2 \,+\, O(s^3)\Big]\,, \\ \mathbf{q}_5 - \mathbf{q}_4 & = & \tfrac{1}{5}\,s^2\,\lambda_f\,\mathbf{t}_f\,. \end{array}$$

Consequently, for any given vector $\mathbf{v}$, we obtain the following expansions

$$\begin{aligned}
[\,\mathbf{q}_1-\mathbf{q}_0,\mathbf{q}_2-\mathbf{q}_1,\mathbf{v}\,] &= \frac{1}{50}\sqrt{30\,\lambda_i\,|\Delta\mathbf{p}|}\;\lambda_i\,[\,\mathbf{t}_i,\mathbf{u}_i(\phi_0),\mathbf{v}\,]\,s^3+O(s^4)\,,\\
[\,\mathbf{q}_2-\mathbf{q}_1,\mathbf{q}_3-\mathbf{q}_2,\mathbf{v}\,] &= \frac{1}{10}\sqrt{30\,\lambda_i\,|\Delta\mathbf{p}|}\;|\Delta\mathbf{p}|\,[\,\mathbf{u}_i(\phi_0),\mathbf{u},\mathbf{v}\,]\,s+O(s^2)\,,\\
[\,\mathbf{q}_3-\mathbf{q}_2,\mathbf{q}_4-\mathbf{q}_3,\mathbf{v}\,] &= \frac{1}{10}\sqrt{30\,\lambda_f\,|\Delta\mathbf{p}|}\;|\Delta\mathbf{p}|\,[\,\mathbf{u},\mathbf{u}_f(\phi_2),\mathbf{v}\,]\,s+O(s^2)\,,\\
[\,\mathbf{q}_4-\mathbf{q}_3,\mathbf{q}_5-\mathbf{q}_4,\mathbf{v}\,] &= \frac{1}{50}\sqrt{30\,\lambda_f\,|\Delta\mathbf{p}|}\;\lambda_f\,[\,\mathbf{u}_f(\phi_2),\mathbf{t}_f,\mathbf{v}\,]\,s^3+O(s^4)\,.
\end{aligned}\tag{42}$$

Now from (15) and (36), we obtain

$$[\,\mathbf{t}_i,\mathbf{u}_i(\phi_0),\mathbf{N}_i\,]=\frac{|\mathbf{u}\times\mathbf{t}_i|}{|\mathbf{u}+\mathbf{t}_i|}\cos\phi_0\,,\qquad [\,\mathbf{u}_f(\phi_2),\mathbf{t}_f,\mathbf{N}_f\,]=\frac{|\mathbf{u}\times\mathbf{t}_f|}{|\mathbf{u}+\mathbf{t}_f|}\cos\phi_2\,,\tag{43}$$

which are both positive quantities under the assumption $\phi_0,\phi_2\in(-\frac{1}{2}\pi,+\frac{1}{2}\pi)$. Using these expressions with the choices $\mathbf{v}=\mathbf{N}_i$ and $\mathbf{v}=\mathbf{N}_f$ in the first and last expansions in (42), respectively, one may verify that for $\phi_0,\phi_2\in(-\frac{1}{2}\pi,+\frac{1}{2}\pi)$ the two inequalities (21) are satisfied asymptotically.

Consider now the conditions under which the inequalities (22) hold asymptotically. From (6), we obtain

$$\begin{aligned}
[\,\mathbf{q}_1-\mathbf{q}_0,\mathbf{q}_2-\mathbf{q}_1,\mathbf{q}_3-\mathbf{q}_2\,] &= \frac{\sqrt{30}}{50}\,(\lambda_i|\Delta\mathbf{p}|)^{3/2}\,[\,\mathbf{t}_i,\mathbf{u}_i(\phi_0),\mathbf{u}\,]\,s^3+O(s^4)\,,\\
[\,\mathbf{q}_2-\mathbf{q}_1,\mathbf{q}_3-\mathbf{q}_2,\mathbf{q}_4-\mathbf{q}_3\,] &= \frac{3}{10}\,\sqrt{\lambda_i\,\lambda_f}\,|\Delta\mathbf{p}|^2\,[\,\mathbf{u}_i(\phi_0),\mathbf{u},\mathbf{u}_f(\phi_2)\,]\,s^2+O(s^3)\,,\\
[\,\mathbf{q}_3-\mathbf{q}_2,\mathbf{q}_4-\mathbf{q}_3,\mathbf{q}_5-\mathbf{q}_4\,] &= \frac{\sqrt{30}}{50}\,(\lambda_f|\Delta\mathbf{p}|)^{3/2}\,[\,\mathbf{u},\mathbf{u}_f(\phi_2),\mathbf{t}_f\,]\,s^3+O(s^4)\,,
\end{aligned}\tag{44}$$

where, setting

$$\delta\;:=\;|\mathbf{t}_i\times\mathbf{u}|\,|\mathbf{u}\times\mathbf{t}_f|\,(\mathbf{N}_i\cdot\mathbf{N}_f)\;=\;(\mathbf{t}_i\times\mathbf{u})\cdot(\mathbf{u}\times\mathbf{t}_f)\,,\tag{45}$$

we have

$$\begin{aligned}
[\,\mathbf{t}_i,\mathbf{u}_i(\phi_0),\mathbf{u}\,] &= -\frac{|\mathbf{u}\times\mathbf{t}_i|^2}{|\mathbf{u}+\mathbf{t}_i|}\sin\phi_0\,,\\
[\,\mathbf{u}_i(\phi_0),\mathbf{u},\mathbf{u}_f(\phi_2)\,] &= \frac{\tau\,\cos\beta-\delta\,\sin\beta}{|\mathbf{u}+\mathbf{t}_i|\,|\mathbf{u}+\mathbf{t}_f|}\,,\\
[\,\mathbf{u},\mathbf{u}_f(\phi_2),\mathbf{t}_f\,] &= \frac{|\mathbf{u}\times\mathbf{t}_f|^2}{|\mathbf{u}+\mathbf{t}_f|}\sin\phi_2\,.
\end{aligned}\tag{46}$$

Consequently, the inequalities in (22) hold asymptotically if ϕ_0, ϕ_2 satisfy the conditions

$$\tau\,\sin\phi_0<0\,,\quad \frac{\delta}{\tau}\,\sin\beta\;<\;\cos\beta\,,\quad \tau\,\sin\phi_2>0\,.\tag{47}$$

Considering also Proposition 1, the above results may be summarized as follows.

Proposition 3. *If the PH quintic spline segments are defined by selecting in each case the angles* $\phi_0, \phi_2 \in (-\frac{1}{2}\pi, +\frac{1}{2}\pi)$ *such that the inequalities in (47) hold, then* $\mathbf{r}(t)$ *asymptotically satisfies the shape–preserving criteria specified in Section 2.*

Thus we can conclude that if $\phi_0, \phi_2 \in (-\frac{1}{2}\pi, +\frac{1}{2}\pi)$ are non–zero, of appropriate sign, and sufficiently small magnitude, the inequalities in (47) are satisfied. Hence, the admissibility region for such ϕ_0, ϕ_2 is non–empty. The following remark completes the present results.

Remark 1. *If* $\tau \neq 0$*, the choice* $\phi_0 = \phi_2 = 0$ *is not admissible. This can be seen as follows. If* $\phi_0 = \phi_2 = 0$*, one must consider higher–order terms to evaluate the asymptotic sign of the first and last expressions on the left in (44). Since, in this case,* $\mathcal{U}_0 = \mathbf{u}_i(0) = \mathbf{n}_i$ *and* $\mathcal{U}_2 = \mathbf{u}_f(0) = \mathbf{n}_f$*, we have*

$$\mathcal{A}_1^{(1)} \;=\; -\tfrac{3}{4}(\mathbf{n}_i + \mathbf{n}_f)\,,$$

and consequently

$$\mathit{vect}(\mathcal{U}_0\,\mathbf{u}\,\mathcal{A}_1^{(1)*}) \;=\; -\tfrac{3}{4}(\mathbf{t}_i{+}\mathbf{e})\,, \qquad \mathit{vect}(\mathcal{A}_1^{(0)}\mathbf{u}\,\mathcal{A}_1^{(1)*}) \;=\; -\tfrac{3}{4}\sqrt{30\,|\Delta\mathbf{p}|}\;(\mathbf{n}_i{+}\mathbf{n}_f)\,.$$

Using the expression for $\mathbf{e}$ *in (20), we then obtain*

$$\begin{aligned}
\frac{1}{\tau}\,[\,\mathbf{q}_1-\mathbf{q}_0, \mathbf{q}_2-\mathbf{q}_1, \mathbf{q}_3-\mathbf{q}_2\,] &= \;-\frac{3|\Delta\mathbf{p}|\,s^4}{50\,|\mathbf{u}{+}\mathbf{t}_i|\,|\mathbf{u}{+}\mathbf{t}_f|}\,(1-\tfrac{1}{4}(1+\mathbf{u}\cdot\mathbf{t}_i)) + O(s^5)\,,\\
\frac{1}{\tau}\,[\,\mathbf{q}_3-\mathbf{q}_2, \mathbf{q}_4-\mathbf{q}_3, \mathbf{q}_5-\mathbf{q}_4\,] &= \;-\frac{3|\Delta\mathbf{p}|\,s^4}{50\,|\mathbf{u}{+}\mathbf{t}_i|\,|\mathbf{u}{+}\mathbf{t}_f|}\,(1-\tfrac{1}{4}(1+\mathbf{u}\cdot\mathbf{t}_f)) + O(s^5)\,.
\end{aligned}$$

Since the highest order term of both these expressions is negative, the choice $\phi_0 = \phi_2 = 0$ *is inadmissible when* $\tau \neq 0$ *if the torsion constraint introduced in Section 2 is required. In fact, since the signs of* $\tau(u_j^+)$ *and of* $\tau(u_{j+1}^-)$ *are the same as those of* $[\,\mathbf{q}_1-\mathbf{q}_0, \mathbf{q}_2-\mathbf{q}_1, \mathbf{q}_3-\mathbf{q}_2\,]$ *and* $[\,\mathbf{q}_3-\mathbf{q}_2, \mathbf{q}_4-\mathbf{q}_3, \mathbf{q}_5-\mathbf{q}_4\,]$*, respectively, they are evidently asymptotically incorrect.*

5.2 Asymptotic behaviour of the CC criterion

We first observe that

$$\lim_{s\to 0}\frac{\mathbf{w}_h}{s^2\sqrt{\lambda_i\lambda_f}} \;=\; \frac{|\mathbf{t}_i\times\mathbf{t}_f|}{\sqrt{(\mathbf{u}\cdot\mathbf{g}^+)^2\,|\mathbf{t}_i\times\mathbf{t}_f|^2 + (\mathbf{u}\cdot\hat{\mathbf{g}})^2\,|\mathbf{t}_i+\mathbf{t}_f|^2}}\,[\,\mathbf{u}-(\mathbf{u}\cdot\mathbf{g}^-)\,\mathbf{g}^-\,]\,, \tag{48}$$

with the assumption that $\mathbf{u} = \Delta\mathbf{p}/|\Delta\mathbf{p}|$. Setting $\beta_L := \lim_{s\to 0}\beta$, we consider the expressions for $\sin\beta_L$ and $\cos\beta_L$ satisfying (25) in this limit, i.e., when the right–hand side of (25) is the limit vector given by (48). Since (25) defines a relation between vectors in the plane Π, and we assume that $\mathbf{t}_i \neq \pm\mathbf{t}_f$, we can reduce (25) to the two scalar equations

$$\begin{aligned}
\tau\,\cos\beta_L \;+\; (1+g_l+g_r+g_c)\,\sin\beta_L \;&=\; \mu\,\tau/(1-g_c)\,,\\
(1+g_l+g_r+g_c)\,\cos\beta_L \;-\; \tau\,\sin\beta_L \;&=\; \mu\,(g_l+g_r)/2\,,
\end{aligned}$$

by considering $(\mathbf{e}\cos\beta + \mathbf{f}\sin\beta)\cdot(\mathbf{t}_i\times\mathbf{t}_f)$ and $(\mathbf{e}\cos\beta + \mathbf{f}\sin\beta)\cdot(\mathbf{t}_i+\mathbf{t}_f)$, respectively, where μ is an immaterial positive value, and we introduce the notations

$$g_l := \mathbf{t}_i\cdot\mathbf{u}\,,\quad g_r := \mathbf{t}_f\cdot\mathbf{u}\,,\quad g_c := \mathbf{t}_i\cdot\mathbf{t}_f\,. \tag{49}$$

Consequently, we have

$$\sin\beta_L = \frac{S}{\sqrt{S^2+C^2}}\,,\quad \cos\beta_L = \frac{C}{\sqrt{S^2+C^2}}\,, \tag{50}$$

where

$$S := \tau\,\frac{(1+g_c)(2+g_l+g_r)}{2(1-g_c)}\,,\quad C := \frac{\tau^2}{1-g_c}+\frac{g_l+g_r}{2}\,(1+g_c+g_l+g_r)\,. \tag{51}$$

This implies that

$$\tau\,\sin\beta_L > 0\,,$$

i.e., the sign of $\sin\beta_L$ is the same as that of the discrete torsion. Furthermore, under the mild assumption

$$g_l+g_r = (\mathbf{t}_i+\mathbf{t}_f)\cdot\mathbf{u} > 0 \tag{52}$$

on the data, we also have

$$\cos\beta_L > 0\,. \tag{53}$$

Now with the choice (34) the unit vector $\mathbf{n}$ in (17) tends to $\mathbf{u}$ as $s\to 0$, and writing $\alpha_L = \lim_{s\to 0}\alpha$, from (30) and (31) we obtain

$$\tan\alpha_L = \rho\,\tan\tfrac{1}{2}\beta\,, \tag{54}$$

where

$$\rho := \lim_{s\to 0}\frac{a}{c} = \frac{\sqrt{\lambda_i}\,(\mathbf{n}_i\cdot\mathbf{u})-\sqrt{\lambda_f}(\mathbf{n}_f\cdot\mathbf{u})}{\sqrt{\lambda_i}\,(\mathbf{n}_i\cdot\mathbf{u})+\sqrt{\lambda_f}(\mathbf{n}_f\cdot\mathbf{u})}\,,$$

and $|\rho|<1$ since (15) implies that $\mathbf{n}_i\cdot\mathbf{u}>0$ and $\mathbf{n}_f\cdot\mathbf{u}>0$. Note that, in the limit $s\to 0$, the inequality on the right of (30) implies that

$$\cos\alpha_L > 0\,, \tag{55}$$

since the coefficients b and d both tend to zero. Thus, considering also (54), this inequality can be written as

$$c_L\,\cos\alpha_L\,(1+\rho^2\tan^2\tfrac{1}{2}\beta_L) > 0\,,$$

where c_L is the positive limit value of c introduced in (31). To show that, in the limit $s\to 0$, the CC criterion yields a PH quintic interpolant whose torsion sign agrees with that of τ, we first prove the following proposition.

Proposition 4. *Setting $\phi_{0,L} := \alpha_L - \frac{1}{2}\beta_L$, $\phi_{2,L} := \alpha_L + \frac{1}{2}\beta_L$, we have*

$$\sin\phi_{0,L}\,\sin\phi_{2,L} < 0\,, \tag{56}$$

with

$$\tau\,\sin\phi_{0,L} < 0\,. \tag{57}$$

Proof : By standard trigonometric addition formulae, it follows that condition (56) holds if and only if $|\cos\alpha_L \sin\frac{1}{2}\beta_L| > |\sin\alpha_L \cos\frac{1}{2}\beta_L|$, i.e.,

$$\tan^2\alpha_L \,<\, \tan^2\tfrac{1}{2}\beta_L\,,$$

which is certainly true, since the absolute value of ρ in (54) is less than one. In order to verify that (57) also holds, we use (54) to write

$$\tau\,\sin\phi_{0,L} \,=\, \tau\,(\sin\alpha_L\cos\tfrac{1}{2}\beta_L - \cos\alpha_L\sin\tfrac{1}{2}\beta_L) \,=\, \gamma\,\sin\tfrac{1}{2}\beta_L\,(\rho-1)\,\cos\alpha_L\,,$$

which verifies (57) since $|\rho| < 1$, $\cos\alpha_L > 0$, $\gamma\,\sin\beta_L > 0$, and $\sin\beta_L\,\sin\frac{1}{2}\beta_L > 0$ (as $\cos\frac{1}{2}\beta_L > 0$). ∎

This proposition indicates that, in the limit $s \to 0$, the first and third inequalities in (47) are satisfied. Now considering (50), the second inequality in (47) implies asymptotically that

$$C \,>\, \frac{\delta}{\tau}\,S\,, \tag{58}$$

where C and S are defined in (51). The following proposition proves that this inequality is satisfied, at least under the assumption (52) and that

$$g_c \,=\, \mathbf{t}_i\cdot\mathbf{t}_f \,>\, 0\,. \tag{59}$$

Proposition 5. *If the data satisfy the conditions (52) and (59), the inequality (58) holds.*

Proof : For brevity we use the notations introduced in (49). Then S can be written as

$$S \,=\, \tau\,\left[\frac{1+g_l+g_c+g_r}{1-g_c} - \frac{g_l+g_r}{2}\right]\,,$$

and noting that the scalar δ introduced in (45) is such that $\delta = g_l\,g_r - g_c$, with some algebra one can obtain

$$C - \frac{\delta}{\tau}\,S \,=\, \frac{\tau^2}{1-g_c} + \frac{g_l+g_r}{2}\,(1+g_l)(1+g_r) \,-\, \frac{(g_l\,g_r-g_c)\,(1+g_l+g_r+g_c)}{1-g_c}\,.$$

Since $g_l+g_r > 0$ and g_l, g_r, g_c are all of absolute value less than 1 for space data, then (58) clearly holds if $g_l\,g_r - g_c \le 0$. On the other hand, if $g_l\,g_r - g_c > 0$, we have $1+g_l+g_r+g_c < (1+g_l)(1+g_r)$, and thus

$$\begin{aligned} C - \frac{\delta}{\tau}\,S \;&>\; \frac{\tau^2}{1-g_c} + \left[\frac{g_l+g_r}{2} - \frac{(g_l\,g_r-g_c)}{1-g_c}\right](1+g_l)(1+g_c) \\ &=\; \frac{\tau^2}{1-g_c} + \frac{(g_l+g_r-2g_lg_r)+g_c(2-g_l-g_r)}{2(1-g_c)}\,(1+g_l)(1+g_c)\,. \end{aligned}$$

Thus, using (59) and the fact that $g_l+g_r > 2g_l\,g_r$ and $g_l+g_r < 2$ (since (52) holds and g_l, g_r are of absolute value less than 1), we see that the inequality (58) holds. ∎

Finally, note that the CC criterion also ensures satisfaction of the prescribed end–point convexity constraints, i.e., the positivity of both $\cos\phi_{0,L}$ and $\cos\phi_{2,L}$. Using standard trigonometric formulae, these conditions are equivalent to $\cos\alpha_L\,\cos\frac{1}{2}\beta_L$ being positive and greater than $|\sin\alpha_L \sin\frac{1}{2}\beta_L|$. Satisfaction of the first requirement is guaranteed by (32) and (55). Furthermore, (53) and (54) ensure that $|\tan\alpha_L\,\tan\frac{1}{2}\beta_L| < 1$, since $\tan\alpha_L = \rho\tan\frac{1}{2}\beta_L$ with $|\rho| < 1$ and $\tan^2\frac{1}{2}\beta_L = (1-\cos\beta_L)/(1+\cos\beta_L)$ with $\cos\beta_L > 0$, and this immediately implies that $\cos\alpha_L\,\cos\frac{1}{2}\beta_L > |\sin\alpha_L \sin\frac{1}{2}\beta_L|$.

The key points of the preceding asymptotic analysis may be summarized as follows.

Proposition 6. *If, in each spline segment, sufficiently small tension parameters are used and the two free angular parameters are selected using the CC criterion, then — under the assumption that the data for each segment satisfy (52) and (59) — the hypothesis of Proposition 3 holds, and the resulting G^1 PH quintic spline Hermite interpolant is shape–preserving in the sense specified in Section 2.*

6 Numerical examples

The implementation of the above procedures is now illustrated through some computed examples. For cases in which the given data are sampled from a smooth analytic curve $\mathbf{c}(u)$, $u \in [\,a,b\,]$ — i.e., $\mathbf{p}_j = \mathbf{c}(u_j)$ and $\mathbf{t}_j = \mathbf{c}'(u_j)/|\mathbf{c}'(u_j)|$ for $j = 0,\ldots,N$ — the spline knots are set equal to the parameter values $u_0,\ldots,u_N$ of the data points. In all other cases, they are assigned using the standard chord–length parameterization, namely $u_0 = 0$ and $u_{j+1} = u_j + |\Delta\mathbf{p}_j|/(|\Delta\mathbf{p}_0| + \cdots + |\Delta\mathbf{p}_{N-1}|)$ for $j = 0,\ldots,N-1$. Also, when the data are sampled from an analytic curve $\mathbf{c}(u)$, the positive parameters λ_i and λ_f for the j–th spline segment are fixed as

$$\lambda_i \;=\; (u_{j+1}-u_j)\,|\mathbf{c}'(u_j)|\,, \qquad \lambda_f \;=\; (u_{j+1}-u_j)\,|\mathbf{c}'(u_{j+1})|\,. \tag{60}$$

Note that this choice implies the normalization

$$\lambda_i^2 + \lambda_f^2 = (u_{j+1}-u_j)^2\,\left(|\mathbf{c}'(u_j)|^2 + |\mathbf{c}'(u_{j+1})|^2\right),$$

while the shape parameter λ_f/λ_i is set equal to the ratio $|\mathbf{c}'(u_{j+1})|/|\mathbf{c}'(u_j)|$.

When the data are not sampled from an analytic curve, the parameter values

$$\lambda_i \;=\; \lambda_f \;=\; u_{j+1}-u_j \tag{61}$$

are used, corresponding to the normalization $\lambda_i^2 + \lambda_f^2 = 2\,(u_{j+1}-u_j)^2$, and the shape parameter λ_f/λ_i is set equal to 1. These choices, together with the assignment of spline knots using the chord–length parameterization, amount to regarding the parameter u as an (approximate) arc length. Furthermore, the tension parameter s is always initially set equal to 1, and is reduced (as little as possible) only when necessary to guarantee satisfaction of the prescribed shape–preserving criteria. Note that, if the tension parameter is equal to 1 in all the

spline segments, both strategies used to select the parameters λ_i, λ_f ensure that the PH spline interpolant is C^1. Specifically, when unit tension parameters are used, we have $\mathbf{S}'(u_j) = \mathbf{c}'(u_j)$ with the first strategy, and $\mathbf{S}'(u_j) = \mathbf{t}_j$ with the second, for $j = 0, \ldots, N$.

For completeness we also mention that, in the experiments, the choice (34) is always used for the unit vector $\mathbf{u}$ in the representation (2). This is immaterial when the CC is adopted ([27]), but is important if the angles (35) are set equal to constant values (e.g., zero), independent of the data. Since the convexity criterion of Section 2 is satisfied in all the experiments described below, the accompanying figures focus on displaying the spline interpolant and its associated torsion plot.

The first example is concerned with non–uniformly sampled data from a circular helix $\mathbf{c}(u) = (\cos u, \sin u, \frac{1}{2}u)$, $u \in [\,0, 4\pi\,]$, which has constant torsion equal to $1/\sqrt{5} \approx 0.45$. It is evident in Fig. 1 that, when α and β are set to zero, the resulting PH spline curve does not satisfy the shape–preserving constraints, since in the seventh segment the sign of the torsion is not everywhere the same as that of the discrete torsion. Note that, according to Remark 1, this defect cannot be remedied by reducing the segment tension parameter if we fix $\alpha = \beta = 0$. If, instead, the CC criterion is used to define α, β the shape–preserving constraints are satisfied even without any reduction of the tension parameter, and the resulting spline curve also exhibits better overall shape — see Fig. 2.

In the second example, the interpolation points are from a benchmark test for shape–preserving spline interpolation, proposed in [20] — see Remark 2 below for the unit tangents. The data specify a symmetric closed curve, with three collinear points and also several coplanar points. Comparing Fig. 3 and Fig. 4, we observe that the PH quintic spline constructed using the CC criterion satisfies the shape–preserving constraints, but the torsion constraint is violated in some segments if it is constructed by setting α and β to zero (again, no tension is used in this example). Note also that the range of variation of the torsion is reduced when the CC criterion is used, and that the "back" of the chair can be made less rounded by a reduction of the tension parameters in the first and last spline segments, if desired. A further point of interest concerning this example is that, for the four segments corresponding to coplanar data, the PH spline segments are precisely planar, when both the choice $\alpha = \beta = 0$ and the CC criterion is used (in fact, the CC criterion yields $\alpha = \beta = 0$ for these segments — see Section 4.3).

The third example is concerned with a single PH quintic segment that interpolates (see case #3 in [12]) the data

$$\begin{array}{lll} \mathbf{p}_i = (0,0,0)\,, & \mathbf{t}_i = \mathbf{v}_i/|\mathbf{v}_i|\,, & \mathbf{v}_i = (0.4,-1.5,-1.2)\,, \\ \mathbf{p}_f = (1,1,1)\,, & \mathbf{t}_f = \mathbf{v}_f/|\mathbf{v}_f|\,, & \mathbf{v}_f = (-1.2,-0.6,-1.2)\,. \end{array} \tag{62}$$

Note that, in this case, condition (52) is not satisfied. For this example, the choice $\alpha = \beta = 0$ clearly does not satisfy the torsion constraint, as seen in Fig. 5, and this remains true as s is reduced. For the CC criterion without tension, the

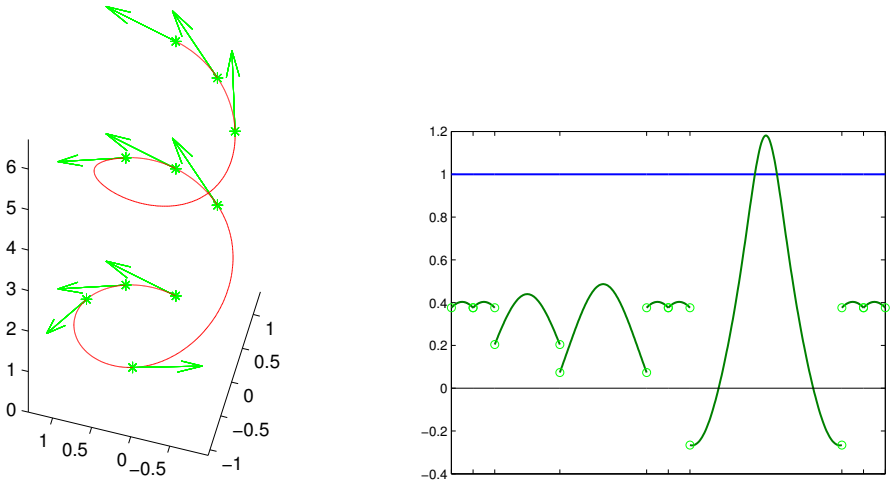

Figure 1: Example 1: Data defined by non-uniform sampling of a circular helix. The PH quintic spline is constructed by setting $\alpha = \beta = 0$ and $s = 1$ in each segment. Left: the resulting PH quintic spline curve (red) together with the given interpolation points and unit tangents (green). Right: the torsion of the PH quintic spline curve (green) and the sign of the discrete torsion (blue).

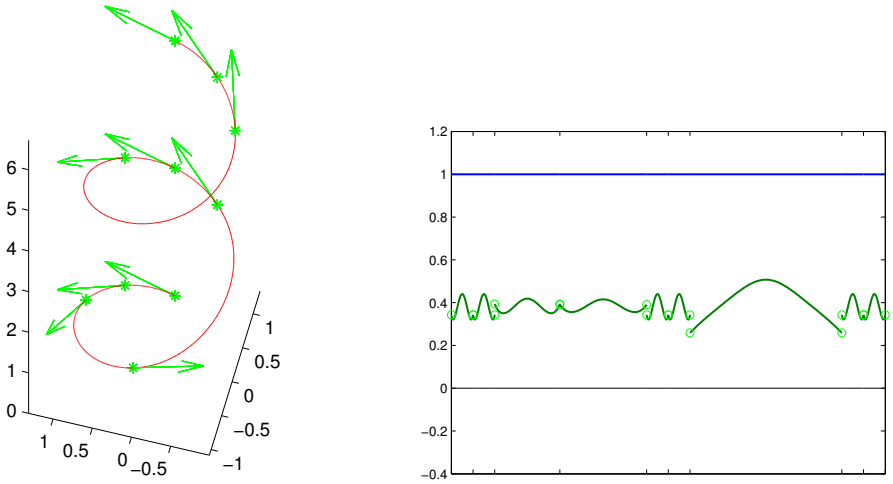

Figure 2: Example 1: Non–uniformly sampled data from a circular helix. The PH quintic spline is constructed by using the CC criterion to define α, β and setting $s = 1$ in each segment. Left: the resulting PH quintic spline curve (red) with the prescribed points and unit tangents (green). Right: the torsion of the PH quintic spline (green) and the sign of the discrete torsion (blue).

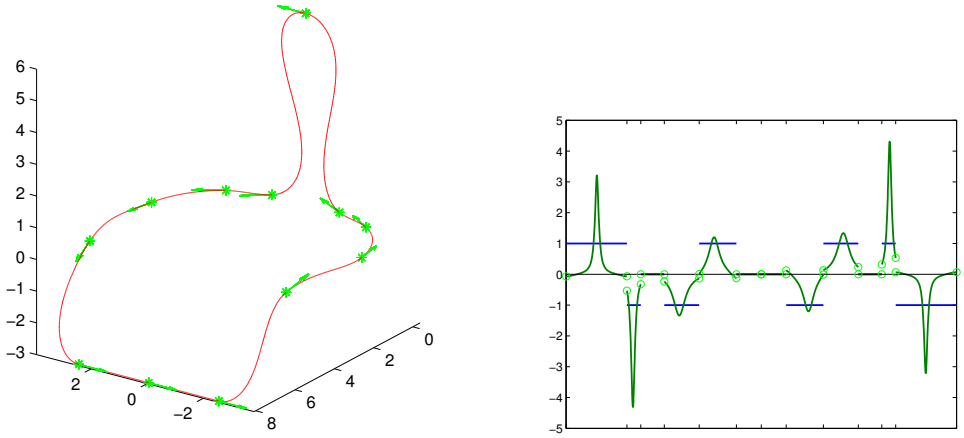

Figure 3: Example 2: The "chair" data from [20]. The PH quintic spline is constructed by setting $\alpha = \beta = 0$ and $s = 1$ in each segment. Left: the resulting PH quintic spline curve (red) with the given points and unit tangents (green), assigned according to (63). Right: the torsion of the PH quintic spline curve (green), and the sign of the discrete torsion (blue).

torsion constraint is mildly violated at one end — see Fig. 6. However, satisfaction of the torsion constraint can be recovered by introducing some tension, as seen in Fig. 7.

In addition to the CC criterion, the alternative HC and BV criteria proposed in [12] for selecting the free angular parameters have also been studied for the data sets described above. It was shown in [12] that these alternative criteria can also be used for general data, and that they also generally produce interpolants of fair shape. For brevity, we present here only a brief summary of the results obtained with these alternative methods. Recall that, like the CC criterion, the HC criterion selects β first, and then α. It differs from CC only in the strategy adopted for choosing β — namely, by maximizing the curve arc length. The BV criterion, on the other hand, selects α and β simultaneously by minimizing[5] $|\,\mathcal{A}_1 - \frac{1}{2}(\mathcal{A}_0 + \mathcal{A}_2)\,|$. Note that the HC and BV criteria have greater computational cost than the CC criterion (BV requires use of a numerical scheme to identify the minimum of a bivariate function, while HC entails determination of the roots of a quartic polynomial).

The experiments indicate that the HC and BV criteria also offer good shape–preserving properties: using the parameter values employed in the case of the CC criterion has produced shape–preserving interpolants in all cases except the first

[5]Equation (30) implies that this quantity is also minimized by the CC and HC criteria, but only with respect to α.

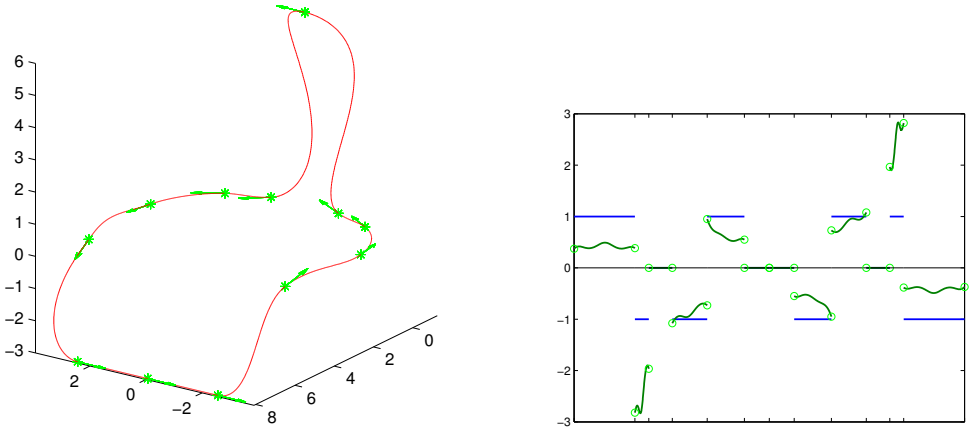

Figure 4: Example 2: The "chair" data from [20]. The PH quintic spline is constructed by defining α, β through the CC criterion and setting $s = 1$ in each segment. Left: the PH quintic spline curve (red) together with the prescribed interpolation points and unit tangents (green), assigned according to (63). Right: the torsion of the PH quintic spline curve (green), and the sign of the discrete torsion (blue). Note that the vertical scale differs from that in Fig. 3.

and last segments of the "chair" data, for which it was necessary to reduce the tension parameter to satisfy the convexity constraints. Although these results are promising, a rigorous proof for the shape–preserving capabilities of the HC or BV criteria is impractical, because closed–form expressions for the α and β parameters are not available in these cases.

Remark 2. *Often, in practice, only the interpolation points* $\mathbf{p}_0, \ldots, \mathbf{p}_N$ *are specified, and a strategy for associating suitable unit tangents with each point must be devised. In particular, it is desirable that this strategy should preserve the shape incidated by the data points, i.e., that the conditions*

$$\begin{aligned} \operatorname{sign}([\,\mathbf{t}_j, \Delta\mathbf{p}_j, \mathbf{t}_{j+1}\,]) &= \operatorname{sign}([\Delta\mathbf{p}_{j-1}, \Delta\mathbf{p}_j, \Delta\mathbf{p}_{j+1}])\,, \\ \operatorname{sign}(\mathbf{N}_{j,i} \cdot \mathbf{N}_{j,f}) &= \operatorname{sign}((\Delta\mathbf{p}_{j-1} \times \Delta\mathbf{p}_j) \cdot (\Delta\mathbf{p}_j \times \Delta\mathbf{p}_{j+1})) \end{aligned} \tag{63}$$

hold for $j = 0, \ldots, N-1$ *(in the case of closed curves with* $\mathbf{p}_0 = \mathbf{p}_N$*, it is assumed that* $\Delta\mathbf{p}_{-1} = \Delta\mathbf{p}_{N-1}$ *and* $\Delta\mathbf{p}_N = \Delta\mathbf{p}_0$*; in the case of open curves,* $\Delta\mathbf{p}_{-1}$ *and* $\Delta\mathbf{p}_N$ *are defined by assigning suitable left and right auxiliary points,* $\mathbf{p}_{-1}$ *and* $\mathbf{p}_{N+1}$*). In fact, in the absence of unit tangents, the discrete quantities defining the shape of the point data are actually the expressions on the right in (63) — as in Example 2. A suitable method for defining unit tangents, proposed in Section 3 of [1], was used to define the unit tangents when the data points* $\mathbf{p}_0, \ldots, \mathbf{p}_N$ *are not derived from a given analytic curve.*

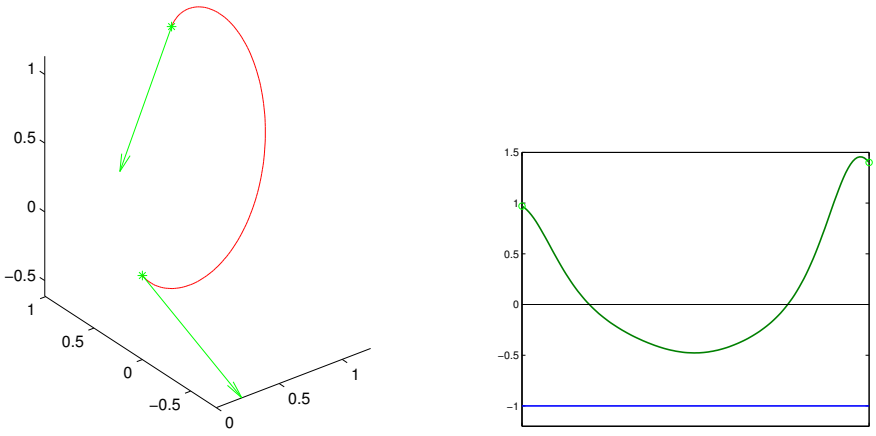

Figure 5: Example 3: A single PH quintic interpolant to the data (62), computed with $\alpha = \beta = 0$ and $s = 1$. Left: the curve (red) with the given points and unit tangents (green). Right: the torsion of the curve (green) and the sign of the discrete torsion (blue).

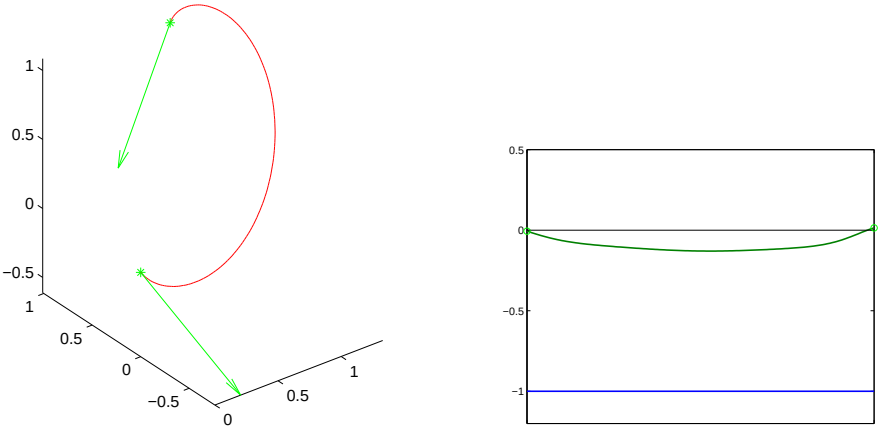

Figure 6: Example 3: A single PH quintic interpolant to the data (62), with $s = 1$ and α, β chosen by the CC criterion. Left: the resulting curve (red) along with the prescribed interpolation points and unit tangents (green). Right: the torsion of the curve (green) and the sign of the discrete torsion (blue). Note that the torsion constraint is marginally violated at $t = 1$.

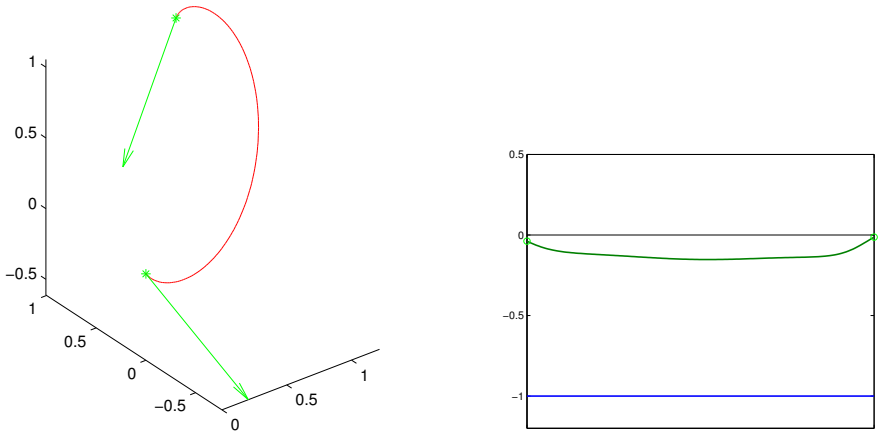

Figure 7: Example 3: A single PH quintic interpolant to the data (62), with $s = 5/6$ and α, β chosen by the CC criterion. Left: the resulting curve (red) together with the prescribed point and unit tangent data (green). Right: the torsion of the curve (green) and the sign of the discrete torsion (blue). Note that the torsion constraint is now satisfied.

Remark 3. *In many applications, G^1 continuity does not suffice, and one must seek interpolants with higher parametric or geometric continuity. If a low–degree spline interpolant is also required, the use of global solution methods is, in general, necessary. C^2 spatial PH quintic splines, for example, require the solution of a global system of equations if they are to interpolate a sequence of points at given knot values. In particular, they incur systems of quadratic equations in quaternion or complex variables — see [16, 14] — and careful initial estimates are required to ensure rapid convergence of iterative solution methods. A possible further extension of the present study involves generalizing the scheme of [14] by introducing tension parameters to relax from C^2 to G^2 smoothness. Such parameters could, in principle, be used to ensure the satisfaction of shape constraints, while still maintaining desirable global shape properties. However, this appears to be a non–trivial problem, since preliminary experiments suggest that, for general data sets, the desired torsion signs cannot be realized by straightforward extension of the initialization strategy employed in [14].*

7 Conclusion

The shape–preserving interpolation of discrete data by space curves is a challenging problem, that has received considerable recent attention in the literature. The shape constraints imposed on space curves are typically concerned with the sign of the torsion, and also the sign of the curvature of certain planar projections of the curve (see [20]). The available shape–preserving interpolation methods — both local and global approaches — are usually *tension schemes*, in which the interpolant depends on parameters that can be used to make the curve converge to the piecewise–linear interpolant. Although the shape constraints are satisfied for a sufficiently strong tension, this degrades the overall fairness of the curve, and may result in extremely large curvature and/or torsion values. Thus, the main goal is to seek a reasonable compromise between shape–preservation and fairness.

Although they offer many useful advantages in applications, the imposition of shape constraints on spatial Pythagorean–hodograph (PH) spline curves is more challenging than for "ordinary" polynomial splines, due to the non–linear nature of the construction algorithms. This study presents the first known scheme for interpolation of spatial data by PH quintic spline curves under shape constraints, based on incorporating a "tension" parameter into each spline segment. In particular, a local G^1 Hermite scheme has been formulated. An asymptotic analysis reveals that a non–empty subset of the parameter space is always compatible with the shape constraints and also that, for "reasonable" data, the CC criterion ([12]) for selecting the free angular parameters on each segment produces interpolants that asymptotically satisfy the prescribed shape constraints. Furthermore, the numerical experiments show that shape preservation is often obtained with no tension or only mild tension and also for more general data than was assumed in the theoretical asymptotic analysis.

The shape constraints considered herein focus on the orientation of the cur-

vature vector at the given interpolation points, and on the sign of the torsion over each spline segment between these points. The investigation of solutions under more general shape constraints and their limiting behavior with respect to the tension parameters, remain challenging open problems, as does the development of schemes that can produce shape–preserving PH splines with higher–order smoothness.

References

[1] S. Asaturyan, P. Costantini, and C. Manni. Local shape–preserving interpolation by space curves. *IMA J. Num. Anal.*, 21:301–325, 2001.

[2] H. I. Choi, D. S. Lee, and H. P. Moon. Clifford algebra, spin representation, and rational parameterization of curves and surfaces. *Adv. Comp. Math.*, 17:5–48, 2002.

[3] P. Costantini, T. N. T. Goodman, and C. Manni. Constructing C^3 shape–preserving interpolating space curves. *Adv. Comp. Math.*, 14:103–127, 2001.

[4] P. Costantini and C. Manni. Shape–preserving C^3 interpolation: the curve case. *Adv. Comp. Math.*, 18:41–46, 2003.

[5] P. Costantini and M. L. Sampoli. Abstract schemes and constrained curve interpolation. In H. Nowacki and P. D. Kaklis, editors, *Creating Fair and Shape–Preserving Curves and Surfaces*, pages 121–130, Leipzig, 1998. Teubner B. G.

[6] P. Costantini and M. L. Sampoli. Constrained interpolation in R^3 by abstract schemes. In M. L. Mazure and L. L. Schumaker, editors, *Curve and Surface Design: Saint-Malo 2002*, pages 93–102, Brentwood, TN, 2003. Nashboro Press.

[7] R. T. Farouki. The conformal map $z \to z^2$ of the hodograph plane. *Comput. Aided Geom. Design*, 11:363–390, 1994.

[8] R. T. Farouki. Pythagorean–hodograph curves. In G. Farin, J. Hoschek, and M. S. Kim, editors, *Handbook of Computer Aided Geometric Design*, pages 405–423. Elsevier, The Netherlands, 2002.

[9] R. T. Farouki. *Pythagorean–Hodograph Curves: Algebra and Geometry Inseparable*. Springer, Berlin, 2008.

[10] R. T. Farouki, M. al Kandari, and T. Sakkalis. Hermite interpolation by rotation–invariant spatial Pythagorean–hodograph curves. *Adv. Comp. Math.*, 17:369–383, 2002.

[11] R. T. Farouki, M. al Kandari, and T. Sakkalis. Strucutral invariance of spatial Pythagorean hodographs. *Comput. Aided Geom. Design*, 19:395–407, 2002.

[12] R. T. Farouki, C. Giannelli, C. Manni, and A. Sestini. Identification of spatial PH quintic Hermite interpolants with near–optimal shape measures. *Comput. Aided Geom. Design*, 25:274–297, 2008.

[13] R. T. Farouki, B. K. Kuspa, C. Manni, and A. Sestini. Efficient solution of the complex quadratic tridiagonal system for C^2 PH quintic splines. *Numer. Algor.*, 27:35–60, 2001.

[14] R. T. Farouki, C. Manni, F. Pelosi, and M. L. Sampoli. Design of C^2 spatial Pythagorean–hodograph quintic splines by control polygons. In M. E. Smith, editor, *Proceedings of the Avignon 2011 Curves and Surfaces Conference*, Lecture Notes on Computer Sciences, pages 253–269, Berlin, 2012. Springer.

[15] R. T. Farouki, C. Manni, and A. Sestini. Shape–preserving interpolation by G^1 and G^2 PH quintic splines. *IMA J. Numer. Anal.*, 23:175–195, 2003.

[16] R. T. Farouki, C. Manni, and A. Sestini. Spatial C^2 PH quintic splines. In T. Lyche, M-L. Mazure, and L. L. Schumaker, editors, *Curve and Surface Design: Saint–Malo 2002*, pages 147–156, Nashville, TN, 2003. Nashboro Press.

[17] T. N. T. Goodman. Total positivity and the shape of curves. In M. Gasca and C. Micchelli, editors, *Total Positivity and Its Applications*, pages 157–186, Dordrecht, 1996. Kluwer.

[18] T. N. T. Goodman. Shape preserving interpolation by curves. In J. Levesley, I. J. Anderson, and J. C. Mason, editors, *Algorithms for Approximation IV*, pages 24–35, Huddersfield, 2002. University of Huddersfield.

[19] T. N. T. Goodman, B. H. Ong, and M. L. Sampoli. Automatic interpolation by fair, shape–preserving G^2 space curves. *Comput. Aided Design*, 30:813–822, 1998.

[20] P. D. Kaklis and M. T. Karavelas. Shape preserving interpolation in R^3. *IMA J. Numer. Anal.*, 17:373–419, 1997.

[21] M. T. Karavelas and P. D. Kaklis. Spatial shape–preserving interpolation using ν–splines. *Numer. Alg.*, 23:217–250, 2000.

[22] C Manni. On shape preserving C^2 Hermite interpolation. *BIT*, 41:127–148, 2001.

[23] F. Pelosi, R. T. Farouki, C. Manni, and A. Sestini. Geometric Hermite interpolation by spatial Pythagorean–hodograph cubics. *Adv. Comp. Math.*, 22:325–352, 2005.

[24] F. Pelosi, M. L. Sampoli, R. T. Farouki, and C. Manni. A control polygon scheme for design of planar C^2 PH quintic spline curves. *Comput. Aided Geom. Design*, 24:28–52, 2007.

[25] R. Renka. Shape-preserving interpolation by fair discrete G^3 space curves. *Comput. Aided Geom. Design*, 22:793–809, 2005.

[26] D. G. Schweikert. An interpolation curve using a spline in tension. *Math. Phys.*, 45:312–317, 1966.

[27] A. Sestini, L. Landolfi, and C. Manni. On the approximation order of a space data dependent PH quintic Hermite interpolation scheme. *Comput. Aided Geom. Design*, 30:148–158, 2013.

[28] Z. Sir and B. Jüttler. Spatial Pythagorean hodograph quintics and the approximation of pipe surfaces. In R. Martin, H. Bez, and M. Sabin, editors, *Mathematics of Surfaces XI*, pages 364–380, Berlin, 2005. Springer.